

RESEARCH

Open Access



MicroRNAs are enriched at COVID-19 genomic risk regions, and their blood levels correlate with the COVID-19 prognosis of cancer patients infected by SARS-CoV-2

Simone Anfossi^{1*†}, Faezeh Darbaniyan^{2†}, Joseph Quinlan¹, Steliana Calin³, Masayoshi Shimizu¹, Meng Chen¹, Paola Rausseo¹, Michael Winters⁴, Elena Bogatenkova⁵, Kim-Anh Do⁶, Ivan Martinez⁴, Ziyi Li⁶, Loredana Antal⁷, Tudor Rares Olariu^{7,8†}, Ignacio Wistuba^{1†} and George A. Calin^{1,9*†}

Abstract

Background Cancer patients are more susceptible to an aggressive course of COVID-19. Developing biomarkers identifying cancer patients at high risk of COVID-19-related death could help determine who needs early clinical intervention. The miRNAs hosted in the genomic regions associated with the risk of aggressive COVID-19 could represent potential biomarkers for clinical outcomes.

Patients and methods Plasma samples were collected at The University of Texas MD Anderson Cancer Center from cancer patients ($N = 128$) affected by COVID-19. Serum samples were collected from vaccinated healthy individuals ($n = 23$) at the Municipal Clinical Emergency Teaching Hospital in Timisoara, Romania. An in silico positional cloning approach was used to identify the presence of miRNAs at COVID-19 risk-associated genomic regions: CORSAIRs (COvid-19 RiSk Associated genomic Regions). The miRNA levels were measured by RT-qPCR.

Results We found that miRNAs were enriched in CORSAIR. Low plasma levels of hsa-miR-150-5p and hsa-miR-93-5p were associated with higher COVID-19-related death. The levels of hsa-miR-92b-3p were associated with SARS-CoV-2 test positivity. Peripheral blood mononuclear cells (PBMC) increased secretion of hsa-miR-150-5p, hsa-miR-93-5p, and hsa-miR-92b-3p after in vitro TLR7/8- and T cell receptor (TCR)-mediated activation. Increased levels of these three miRNAs were measured in the serum samples of healthy individuals between one and nine months after the second dose of the Pfizer-BioNTech COVID-19 vaccine. SARS-CoV-2 infection of human airway epithelial cells influenced the miRNA levels inside their secreted extracellular vesicles.

Conclusions MiRNAs are enriched at CORSAIR. Plasma miRNA levels can represent a potential blood biomarker for predicting COVID-19-related death in cancer patients.

[†]Simone Anfossi and Faezeh Darbaniyan contributed equally to this work.

[†]Tudor Rares Olariu, Ignacio Wistuba and George A. Calin senior authors.

*Correspondence:

Simone Anfossi
sanfossi@mdanderson.org
George A. Calin
gcalin@mdanderson.org

Full list of author information is available at the end of the article



Keywords MiRNAs, Genomics, Cancer, COVID-19, SARS-CoV-2, Plasma biomarkers

Introduction

Critical illness of coronavirus disease 2019 (COVID-19) is associated with host-mediated lung inflammation [1], and severe cases progress to acute respiratory distress syndrome (ARDS) [2, 3]. ARDS is characterized by difficulty breathing and low blood oxygen that may cause respiratory failure and is responsible for 70% of fatal COVID-19 cases [4]. Besides the direct cytopathic effect of viral infection, the severity of the disease can be due to the host's response. Indeed, a dysfunctional immune response to the severe acute respiratory syndrome coronavirus 2 (SARS-CoV-2) infection can lead to a massive release of cytokines (cytokine storm) and sepsis-like symptoms that cause inflammation-induced injuries to tissue and blood vessels of the lung [1] and also multi-organ failure [4, 5]. Patients with cancer generally have a greater risk of unfavorable outcomes from COVID-19, with higher age, male sex, and cancer type (blood cancer) as the main risk factors [6]. Furthermore, host genetic factors can be associated with the susceptibility to developing severe COVID-19 and, therefore, may help identify molecular targets and develop biomarkers to predict clinical outcomes. Over the past three years, genome-wide association studies (GWAS) have identified several genetic variants, such as single nucleotide polymorphisms (SNPs), associated with the severity and susceptibility of COVID-19 [7–9]. Protein-coding genes near these SNPs play essential regulatory functions in immune responses and viral infection [8, 10, 11]. Our study applied a similar but alternative target identification strategy by focusing on a specific class of small non-coding RNAs, the microRNAs (miRNAs), instead of protein-coding genes. In particular, we used a similar approach that allowed us to successfully achieve the initial identification of miRNAs as essential genes for cancer [12]. Our previous study showed that miRNA genes are frequently located at fragile sites, minimal regions of loss of heterozygosity, minimal regions of amplification (minimal amplicons), or common breakpoint regions. In the current study, we assessed the presence of miRNAs in the proximity of the loci harboring the SNPs associated with COVID-19 severity and susceptibility.

MiRNAs are essential regulators in biological processes of immunity, inflammation, cytokine storm, infection, and sepsis [13–15]. Activated immune cells, such as T lymphocytes [16–18], macrophages [19], and dendritic cells [20], can secrete extracellular vesicles (EVs) loaded with miRNAs into the extracellular space. These miRNAs

can reach the blood circulation and be detected by currently used molecular biology techniques [21, 22] as circulating miRNAs with the potential to serve as valuable biomarkers to predict clinical outcomes of cancer patients [22]. In this study, we hypothesized that 1) miRNAs are located in the proximity of SNPs associated with COVID-19 severity and susceptibility, and 2) these specific miRNAs could be detected in the blood of cancer patients affected by COVID-19 and used to predict their prognosis.

Methods

Cohorts and patients

The cancer patients were enrolled at The University of Texas MD Anderson Cancer Center (UT-MDACC) under the APOLLO (Adaptive Patient-Oriented Longitudinal Learning and Optimization) program (protocol 2014–0938) starting from April 15, 2020, to provide COVID-19 whole blood samples that were processed and store at the Institutional Tissue Bank (ITB), a Divisional section of UT-MDACC. We used plasma samples from 218 patients for a total of 410 plasma samples, where 218 samples were collected at the time of enrollment ($t=0$), corresponding to the time of the first positive COVID-19 test, and the remaining 192 samples at different follow-up time points. The demographic characteristics are shown in Table 1. We used ITB plasma samples starting from patients enrolled in May 2020. Individual patients provided one or multiple plasma samples during the follow-up time while affected by COVID-19 and at the time of recovery. Based on the year of sample collection, patients were divided into two cohorts (2020 and 2021). Clinical outcomes were collected for those patients involved in our study, with the follow-up time censored at the time of death or at the end of our study on April 2022 (follow-up time interval: 5 to 23 months).

Twenty-three vaccinated individuals were selected from a group of 92 Romanian healthcare workers in whom the SARS-CoV-2 antibody response to the BNT162b2 mRNA COVID-19 vaccine (Pfizer-BioNTech, Mainz, Germany) was previously assessed [23]. The 23 individuals were healthcare workers from the Municipal and County Clinical Emergency Teaching Hospitals in Timisoara, Romania. All participants were healthy individuals with no associated comorbidities and were not infected with SARS-CoV-2 during the study period, February 26 to November 26, 2021. Each participant was vaccinated with two doses of the Pfizer-BioNTech vaccine at the time of enrollment in the study [24].

Table 1 Demographics and clinical characteristics of COVID-19 patients

Demographics	Characteristics	N=218
Age	13—45	49
	46—59	102
	> 60	67
Sex	Male	119
	Female	99
Race	White	146
	Black or African American	35
	Hispanic	27
	Asian	9
	Native Hawaiian	0
	American Indian or Alaska Native	1
Comorbidities	CC + Diabetes	53
	CC + CVD / HTN	99
	CC + Chronic Respiratory Disease	20
	Only CC	98
Severity	No symptoms	87
	Upper respiratory symptoms	132
	CT pneumonia	102
	ARDS	38
Targeted^a COVID-19 treatment	YES	82
	NO	136
O₂ supplementation	None	150
	Non-invasive / Nasal cannula / Mask	54
	Invasive / Mechanical ventilation	14
Dead /Alive	Dead	47
	Alive	171
Dead	COVID-19-related	20
	Non-COVID-19-related	27
Types of cancer	Solid singles	116
	Solid multiple	13
	Liquid singles	75
	Mixed (solid and liquid)	14

^a Targeted COVID-19 treatment: Remdesivir + antibiotic + corticosteroid ± COVID-19 convalescent plasma

CC Cancer, CVD Cardio-vascular disease, HTN Hypertension; CT pneumonia pneumonia diagnosed by computer tomography ARDS Acute respiratory distress syndrome

Blood sample collection

The blood was drawn according to protocol 2014–0938 from cancer patients at UT-MDACC. Whole blood samples were collected in green top tubes (heparin) and processed by the Diagnostic Blood Processing CORE Laboratory (UT-MDACC) following the Standard Operating Procedure (SOP) of the institution and stored at the ITB. Briefly, whole blood was centrifugated at 2000 rpm

(863xg) for 15 min at room temperature, and the collected plasma was stored in aliquots of 500 µl/vial at -80 °C.

The blood of the vaccinated healthy individuals was drawn monthly at the Municipal Clinical Emergency Hospital in Timisoara, Romania, starting one month after each participant received the second dose of the Pfizer-BioNTech vaccine. The whole blood was collected in red top tubes and centrifugated at 2000 rpm (863xg) for 10 min at room temperature. The collected serum samples were kept in 500 µl/vial aliquots at -20 °C until tested at the Clinical Laboratory of the Municipal Clinical Emergency Teaching Hospital in Timisoara, a reference laboratory for COVID-19 testing in Romania.

Serologic tests

We investigated serum samples collected at one month, three months, six months, and nine months after each participant received the second dose of the Pfizer-BioNTech vaccine. To evaluate the vaccine-elicited antibody response, the SARS-CoV-2 IgG II Quant assay (Abbott, Diagnostics Division, Sligo, Ireland), a chemiluminescent microparticle immunoassay (CMIA) with a sensitivity of 98.1% and specificity of 99.6% [25], was used to detect the SARS-CoV-2 anti-spike (S) protein IgG levels in the serum samples. The IgG levels were measured using the Abbott Alinity i (Abbott Laboratories, Lake Bluff, IL, USA), and those with a cutoff ≥ 50.0 AU/mL were considered positive for IgG [25]. Serologic test kits, including controls, were used according to the protocol specified by the manufacturer, and the results were interpreted based on the manufacturer's criteria.

Selection of miRNA locations at COVID-19 risk-associated genomic regions (CORSAIR)

PubMed search using “SNPs and COVID-19” as keywords and Google search using “COVID-19 genomics”, “non-coding genome, outcome, SARS-CoV-2 infections, SNPs” allowed the collection of publications on SNPs related to COVID-19 risk and differential outcomes. The locations of the SNPs (NCBI human genome resources <https://www.ncbi.nlm.nih.gov/>) were compared with the locations of miRNAs (miRbase <https://mirbase.org/>) using the hg38 reference genome. SNPs were assigned to a miRNA if they were located within 1 Mb up- or downstream of the start position of the miRNA sequence. R was used to extract and compile all experimentally validated target genes of the selected miRNAs from the following databases: miRecords, miRWalk 2.0, miRTarBase, and DIANA-TarBase v8.

Statistical analyses

Unless otherwise specified, all statistical comparisons between two groups were calculated based on the Mann–Whitney U test.

We also developed a prognostic model to predict time to death related to SARS-CoV-2 infection and COVID-19 on 106 patient samples. In addition, the Concordance c-index and AUC at each time point were evaluated on an independent set of 45 patients. This study has deaths due to other causes that precluded COVID-19-related death. Therefore, alternative causes of death were considered as competing risk events. We performed three separate analyses for predicting the survival: 1) Cause-Specific Hazard (CSH) model for COVID-19-related death (where other causes of death were considered as censoring events), 2) CSH model for non-COVID-19 death (where COVID-19-related deaths were regarded as a censoring event), and 3) sub-distributional hazard model of cumulative incidence function for COVID-19-related death using Fine and Gray Method [26, 27]. Gray's test compared two curves in a cumulative incidence plot to assess the statistical significance [28]. We next developed a prognostic model to predict the time to death due to COVID-19 on the training set. The Concordance c-index and AUC at each time point were evaluated in training and testing groups. All analyses were performed using R version 4.2.0 and CRAN packages "cmprisk" and "survival".

Results

MiRNA are enriched at COVID-19 risk-associated genomic regions (CORSAIR)

We created a GWAS database containing information on the SNPs associated with COVID-19 risk of disease and aggressivity from over 100,000 individuals collected from papers published between October 2020 and January 2022 (Additional Table S1). These papers reported 67 different SNPs located on 20 genomic regions in 19 autosomal chromosomes (except chromosomes 7, 13, and 18) and the sex X chromosome that were associated with different clinical characteristics of COVID-19, such as susceptibility to SARS-CoV-2 infection, COVID-19 disease severity, severe COVID-19 with respiratory failure or protection against severe disease. We evaluated the presence of miRNAs in the proximity of these genomic regions harboring the SNPs associated with COVID-19 risk of illness and aggressivity. Mainly, we investigated genomic regions spanning up to 1 megabase (Mb) up- and down-stream of the COVID-19 risk-associated SNPs (total up to 2Mbs), and we named these regions **CO**vid-19 **Ri**Sk **A**ssociated **R**egions (CORSAIR). The 1 Mb threshold is similar to the one we used to identify the cancer-related miRNA locations in cancer-associated

genomic regions (CAGRs) [12], as this is the distance in which several regulatory elements (such as enhancers) are functionally active [29]. We found that CORSAIR were enriched with miRNAs with 157 miRNA loci identified (Additional Table S2 and S3). Interestingly, a high density of miRNA loci (41 out of the 157 miRNAs, ~26%) was located in the CORSAIR of chromosome 19 (Chr19), one of the smallest chromosomes [30]. Furthermore, none of the 157 miRNAs were located in the chromosome 19 miRNA cluster (C19MC) at the chromosomal band 19q13.42, the largest cluster of human miRNAs expressed in cells during early embryonic development but not in adult tissues except the placenta [31]. This evidence might suggest that the density and specific genomic locations of miRNAs in CORSAIR may be relevant to COVID-19 risk. Therefore, we investigated whether or not this miRNA enrichment in CORSAIR was a random finding. We used the Random Effect Poisson Regression Model to evaluate the association between miRNA locations and CORSAIR and disease aggressivity across different chromosomes. Under this model, the genomic regions were defined as separate windows of the segmented genome with 2 Mb in size. The events were defined as the number of miRNAs located at each region. The fixed effect in the model was the incidence of SNPs in each region. Because different chromosomes have different genetic characteristics that are generally correlated within each chromosome, we considered chromosomes as a random effect. To further investigate the impact of region size on the results, we performed sensitivity analysis by evaluating the results with window sizes ranging from 40 kb to 4 Mb. We reported the incidence rate ratio (IRR), the 95% confidence interval (CI) of the IRR, and the corresponding *P* values to test the hypothesis that the IRR is 1.0 (Fig. 1A). By increasing the size of the region window, we observed shorter confidence intervals with significant *P* values for the IRR of SNP in each model. In contrast, the lengths of the confidences stay stable afterward. To confirm that other genomic features do not confound the findings, we further investigated the effect of SNPs on predicting the number of non-coding ultra-conserved elements (ncUCEs) [32]. Our analysis yielded a non-significant association between SNPs and ncUCEs ($P=0.096$), with an IRR of 0.91, suggesting that ncUCEs distribution is independent of SNP position (Additional Figure S1A). In contrast, miRNAs and SNPs were significantly associated with an IRR of 2.51 ($P=2.5E-9$) (Additional Figure S1B). These data suggest that miRNAs located in proximity to SNPs and associated with COVID-19 risk of disease and aggressivity, which we defined as CORSAIR miRNAs (Fig. 1B), may have a potential correlation with COVID-19.

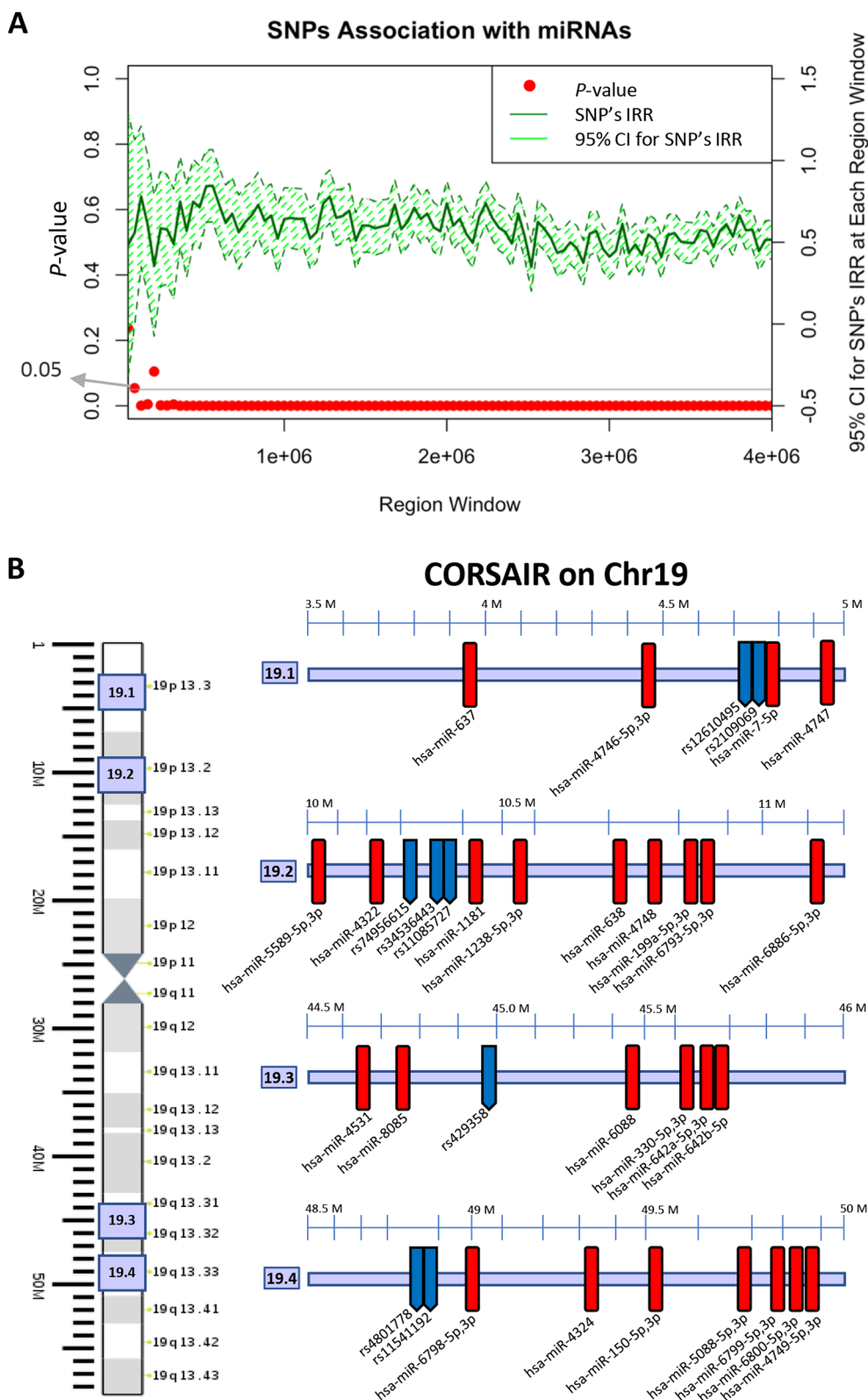


Fig. 1 Association of genomic location between SNPs and miRNAs. **A** SNPs are associated with miRNA genomic location using genome windows of different sizes. The genome windows grow wider from left to right, and the confidence intervals narrow. The association is consistently significant, and the length of confidence interval stables after the genome window reaches ~ 1 Mb. **B** An example of CORSAIR on chromosome 19, where an enrichment of miRNAs (in red) is present in the genomic location around SNPs (in blue)

Selection of CORSAIR miRNAs to be tested in the plasma of cancer patients affected by COVID-19

We investigated the potential association of the 157 CORSAIR miRNAs with COVID-19 risk of disease and aggressivity. Because SARS-CoV-2 infection is characterized by a dysfunctional immune response causing cytokine storm, we first evaluated if the CORSAIR miRNAs are expressed in five immune cell types: monocytes/macrophages (CD14), granulocytes (CD15), B lymphocytes (CD19), T lymphocytes (CD3), and NK cells (CD56) [33]. Among the CORSAIR miRNAs expressed in immune cells, hsa-miR-150-5p had the highest expression in B and T lymphocytes and NK cells (Additional Table S4a). Then, we found that hsa-miR-150-5p had the highest expression levels in the normal lung tissue (Additional Table S5). The hsa-miR-150-5p gene is located in proximity with rs4801778, whose lead variant is significantly associated with reported SARS-CoV-2 infection and in linkage-disequilibrium with the missense variant rs11541192 [34]. Furthermore, hsa-miR-150-5p was the first miRNA to be identified as differentially expressed in patients with sepsis and correlate with the IL-18 expression [35], a cytokine associated with COVID-19 aggressivity [36, 37]. Because of the large number of CORSAIR miRNAs, we decided to reduce the number of selected miRNAs to be tested in the plasma of cancer patients based on their reported expression in 1) miRBase (Additional Table S3), 2) immune cells (Additional Table S4a) and 3) normal lung tissue (Additional Table S5). Because COVID-19-related deaths can be associated with sepsis-like symptoms due to cytokine storm in response to the infection [1, 4, 5, 38, 39], and hsa-miR-150-5p is both a CORSAIR and sepsis-related miRNA, we decided to include in our study five sepsis-related non-CORSAIR miRNAs according to our previous and current investigations [35, 40, 41]: hsa-miR-23a-3p; hsa-miR-26b-5p; hsa-miR-182-5p; hsa-miR-486-5p; and hsa-miR-93-5p. The final list of twenty-three miRNAs included eighteen CORSAIR and five sepsis-related miRNAs that were measured in the plasma of cancer patients (Additional Table S6a).

Levels of miRNAs in the plasma of cancer patients affected by COVID-19 are associated with survival

Because they are easily measurable in the blood, circulating miRNAs may represent helpful biomarkers to assess the clinical outcome of COVID-19 patients at high risk for poor clinical outcomes, such as cancer patients. This is of great importance for high-risk COVID-19 cancer patients, such as patients who are not vaccinated or cannot be vaccinated for COVID-19, because they have a two-fold increased risk of unfavorable outcomes (mortality, intensive care unit admission and severity of

COVID-19) compared with COVID-19 patients without cancer [42].

We evaluated whether the selected miRNAs could be detected in the plasma of cancer patients affected by COVID-19. Only fourteen of the selected twenty-three miRNAs were detected in the plasma samples (Additional Table S6a). Then, we assessed if the levels of detectable miRNAs were associated with patients' clinical outcomes. The patients were divided into three groups: alive (recovered from COVID-19 within three months and alive for at least six months); dead from COVID-19 or COVID-19-related causes (within three months); dead from non-COVID-19-related causes (within three months). The time was counted from the first positive COVID-19 test. We found that patients who died from COVID-19-related causes had significantly lower median hsa-miR-150-5p plasma levels compared with alive patients ($P < 0.0001$) and compared with patients who died from non-COVID-19-related causes ($P = 0.0072$). (Fig. 2A left). Then, we tested the sepsis-related miRNAs. Patients who died from COVID-19-related causes had significantly lower median hsa-miR-93-5p plasma levels compared with alive patients ($P = 0.0017$) and compared with patients who died from non-COVID-19-related causes ($P = 0.0117$) (Fig. 2A center). We repeated these measurements in two independent tests and assessed the reproducibility of the measurements (Ct values) of both hsa-miR-150-5p and hsa-miR-93-5p (Additional Figure S2). We also evaluated if plasma miRNA levels were associated with the positivity status of SARS-CoV-2 infection. In a pair-matched set of patients ($N = 10$), we compared the levels of miRNAs in samples collected after the last SARS-CoV-2 positive test (range 2–12 days) with those of the first sample collected after the negative SARS-CoV-2 test (range 0–23 days). Among the twenty-three tested miRNAs, we found that the levels of hsa-miR-92b-3p significantly decreased in patients who became negative for SARS-CoV-2 infection ($P = 0.0059$) (Fig. 2B). We found no significant results for the other miRNAs (not shown).

These results indicate that low levels of hsa-miR-150-5p and hsa-miR-93-5p measured in the plasma of cancer patients at the beginning or early stage of COVID-19 ($t = 0$) were associated with adverse outcomes during COVID-19 disease compared with patients with higher levels of hsa-miR-150-5p and hsa-miR-93-5p. Finally, the decrease of hsa-miR-92b-3p plasma levels could be associated with the recovery from SARS-CoV-2 infection.

CORSAIR miRNAs are expressed in immune cells and detected in their cell culture supernatants

Both hsa-miR-150-5p and hsa-miR-93-5p are highly expressed in immune cells. In particular, hsa-miR-150-5p has the highest expression in NK, B, and T cells, whereas

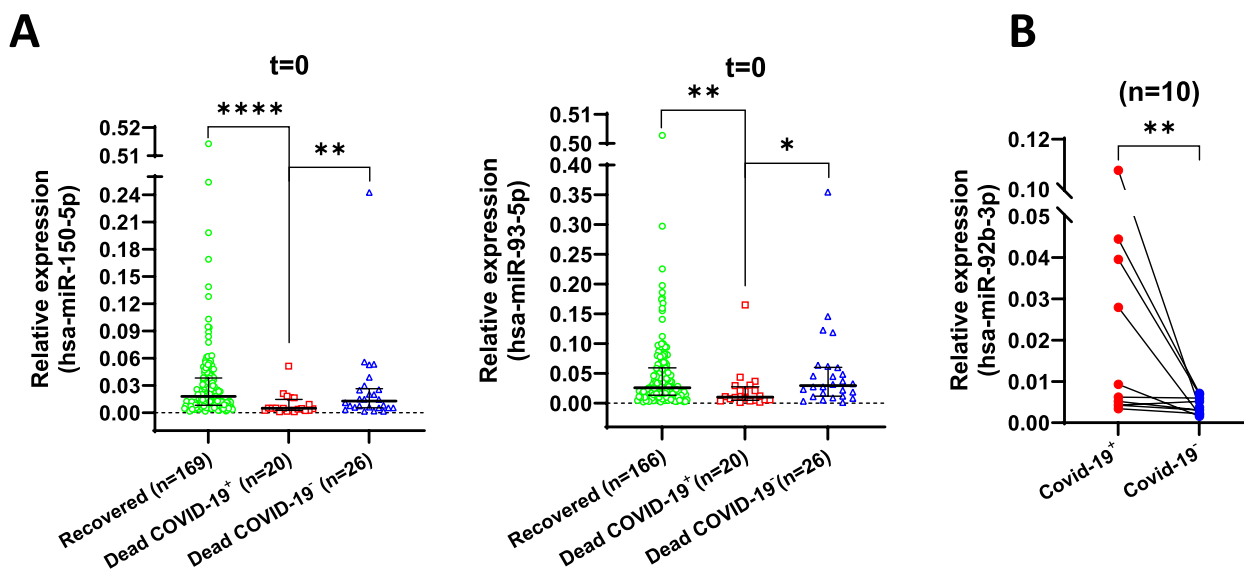


Fig. 2 Expression levels of hsa-miR-150-5p, hsa-miR-93-5p, and hsa-miR-92b-3p in the plasma of cancer patients collected at the time of enrollment ($t=0$). **A** Low levels of both hsa-miR-150-5p and hsa-miR-93-5p were measured in patients who died from COVID-19 or COVID-19-related reasons (Dead COVID-19⁺). Both miRNAs had lower levels in patients who died from COVID-19-related causes (Dead COVID-19⁺) than in alive patients (Recovered) and patients who died from non-COVID-19-related causes (Dead COVID-19⁻). Some samples did not have RT-qPCR amplification signal: hsa-miR-150-5p ($n=2$) and hsa-miR-93-5p ($n=5$) in the Recovered group, hsa-miR-150-5p ($n=1$) and hsa-miR-93-5p ($n=1$) in the Dead COVID-19⁺ group; **B** In pair-matched samples ($n=10$), the levels of hsa-miR-92b-3p correlated with COVID-19 test positivity (Wilcoxon test) P value summary: * <0.05 ; ** <0.01 ; *** <0.001 ; **** <0.0001

hsa-miR-93-5p has the highest expression in monocytes and neutrophils (Additional Table S4a). Because miRNA expression in immune cells can be modulated after their activation [43, 44], miRNAs can be secreted into extracellular space [17, 45] and reach blood circulation, we hypothesized that miRNAs we measured in patients' plasma could be secreted by activated immune cells during SARS-CoV-2 infection and the different levels of secreted miRNAs could reflect modulation in the immune cell activation levels. We used two potent activators to stimulate peripheral blood mononuclear cells (PBMC) from four normal donors. Resiquimod (R848) selectively binds to TLR7/8 receptors, activated by viral ssRNAs in antiviral immune responses, and activates monocytes/macrophages and dendritic cells. Concanavalin A (conc A), a lectin with potent antigen-independent

mitogenic activity, activates T lymphocytes. We measured a differential expression of all the selected fourteen miRNAs in the PBMC six days after activation (Fig. 3A and Additional Figure S3A). We found a modulation of the selected fourteen miRNAs in PBMC at day six and in the supernatants at day three and day six after stimulation (Fig. 3A-B, Additional Figure S3A-B, and Additional Table S6b). Interestingly, hsa-miR-93-5p levels had the highest fold-change increase (around ninefold) in the supernatants six days after conc A activation, whereas hsa-miR-150-5p levels had the third highest fold-change increase (around threefold) in the supernatants six days after R848 activation. The hsa-miR-92b-3p levels had the second highest fold-change increase (around 2.5-fold) in the supernatants three days after conc A activation (Fig. 3B and Additional Table S6b). Finally, we assessed

(See figure on next page.)

Fig. 3 Levels of miRNAs in activated peripheral blood mononuclear cells (PBMC), their supernatants, and in serum samples of Pfizer-BioNTech vaccinated healthy individuals. **A** Variation of the expression levels of hsa-miR-92b-3p, hsa-miR-150-5p, and hsa-miR-93-5p in PBMC at six days after activation with TLR-7/8 agonist (α TLR7/8), T cell mitogen concanavalin A (conc A), compared with unstimulated PBMC; **B** Variation of the expression levels of secreted hsa-miR-92b-3p, hsa-miR-150-5p, and hsa-miR-93-5p into the supernatants of PBMC at three and six days after activation with α TLR7/8, conc A, compared with supernatant of unstimulated PBMC; **C** Variation of hsa-miR-92b-3p, hsa-miR-150-5p, and hsa-miR-93-5p levels in the serum samples of healthy individuals ($n=23$) collected at one, three, six, and nine months after the administration of the second dose of the Pfizer-BioNTech vaccine; **D** Variation of hsa-miR-92b-3p, hsa-miR-150-5p, and hsa-miR-93-5p levels in the pair-matched serum samples of healthy individuals at different times after the administration of the second dose of the Pfizer-BioNTech vaccine. (In **A** and **B**, Unpaired t-test. P value summary: * <0.05 ; ** <0.01 ; *** <0.001 ; **** <0.0001 ; ns not significant; in **D**, Wilcoxon test)

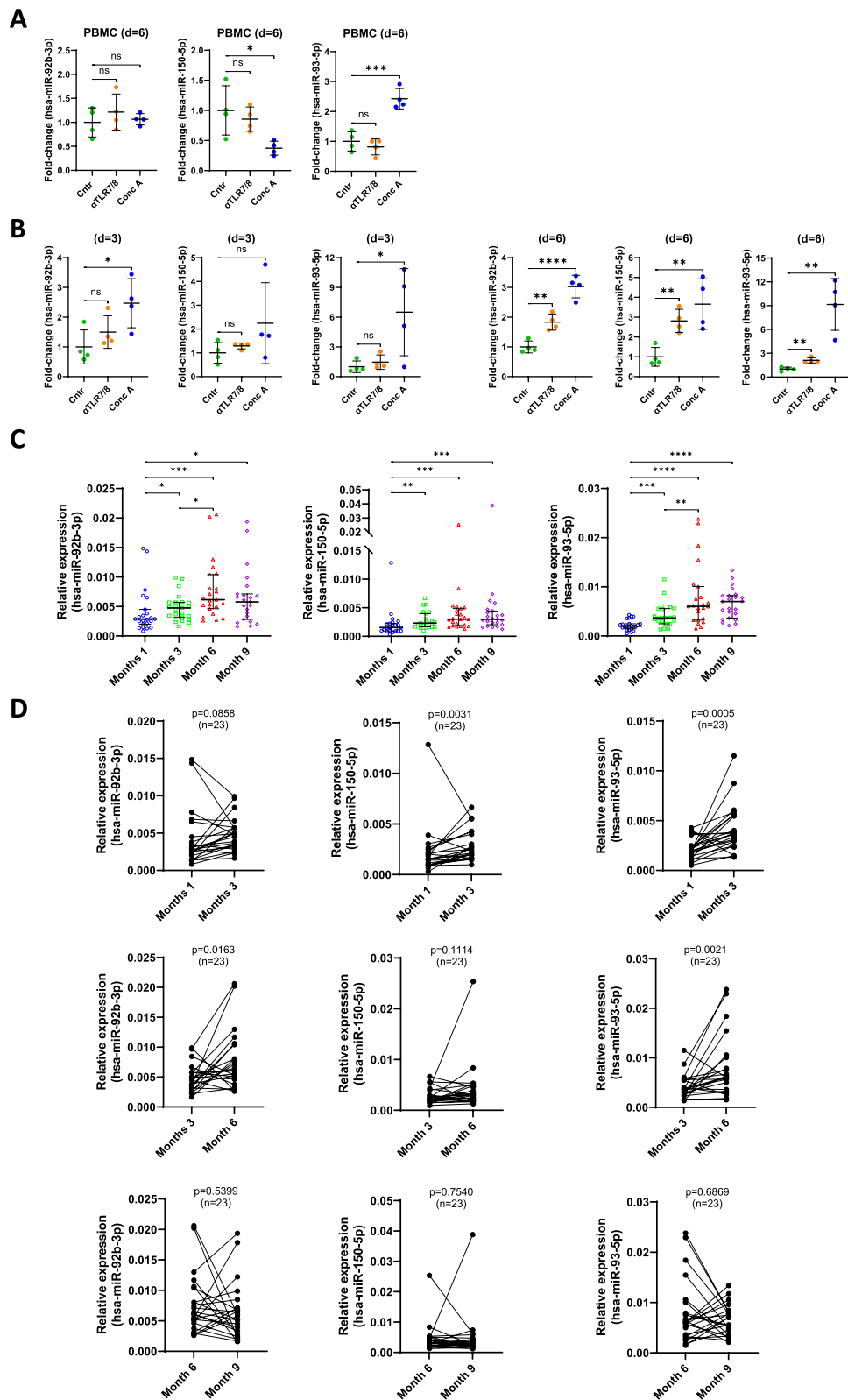


Fig. 3 (See legend on previous page.)

the levels of these three miRNAs in the serum samples collected from 23 healthy individuals at one, three, six, and nine months after the second dose of the Pfizer-BioNTech vaccine. The median serum levels of hsa-miR-93-5p increase progressively up to month nine, whereas those of hsa-miR-92b-3p and hsa-miR-150-5p reached the plateau at month six (Fig. 3C). When we performed a pair-matched analysis, we observed a similar trend, with most healthy individuals having the serum levels of all three miRNAs increasing significantly between month one and month three. In contrast, only hsa-miR-92b-3p and hsa-miR-93-5p continued to increase considerably between month three and month six in most of the healthy individuals. No significant difference was measured between months six and nine (Fig. 3D). We measured an overall increase of the three miRNAs at months six and nine compared with month one (Additional Figure S3C). We measured high levels of SARS-CoV-2 anti-spike (S) protein IgG (>50.0 AU/mL) at month one as a measure of the response to the Pfizer-BioNTech vaccine (Additional Figure S3D). SARS-CoV-2 anti-spike (S) protein IgG levels decreased over time but remained above the limit (>50.0 AU/mL) up to month nine.

We can conclude that increased levels of hsa-miR-92b-3p, hsa-miR-93-5p, and hsa-miR-150-5p secreted into the cell supernatant can be associated with the activation of PBMC by in vitro stimulation and their increased serum levels over time can be associated with the response to anti-COVID-19 vaccine.

CORSAIR and non-CORSAIR miRNAs and their immune cell-related signaling pathways

Then, we investigated the targets and potential pathways regulated by CORSAIR and non-CORSAIR miRNAs by Gene Set Enrichment Analysis (GSEA). Among the 1,167 miRNAs (CORSAIR and non-CORSAIR) expressed in the immune cells, we selected those whose expression exceeded one standard deviation, referred to as “high” (Additional Table S4a). We identified the target genes and the regulated pathways by selected CORSAIR ($n=4$) and non-CORSAIR ($n=139$) miRNAs (Additional Table S4b, c, d, e). After setting the p -value cutoff = 0.05, we found the TGF-beta-signaling pathway to be the top Hallmark pathway regulated by the four CORSAIR miRNAs (Additional Figure S4A and Additional Table S4c). Conversely, the TNF-a-signaling-via-NFkB pathway was the top Hallmark pathway regulated by the 139 non-CORSAIR miRNAs (Additional Figure S4B and Additional Table S4e). Of note, hsa-miR-150-5p can target seven out of the eleven genes regulating the TGF-beta-signaling pathway, and hsa-miR-93-5p can target 64 out of the 199 genes regulating the TNF-a-signaling-via-NFkB pathway (Additional Table S4f). These results supported

the evidence that differential levels of miRNAs hsa-miR-150-5p and hsa-miR-93-5p detected in the plasma of patients with different clinical outcomes can be associated with immune cell functions during COVID-19.

Levels of selected CORSAIR miRNA in the extracellular vesicles secreted by human airway epithelial cells are affected by SARS-CoV-2 infection

We wanted to assess whether miRNAs in the plasma of cancer patients affected by COVID-19 could also originate from the lung epithelial cells during the SARS-CoV-2 infection. We infected NuLi-1 (human bronchus airway epithelium) and HBEC3-KT (normal immortalized human bronchial epithelium) cells with the original SARS-CoV-2 Washington (USA-WA1/2020) strain and the variant SARS-CoV-2 UK (Alpha/B.1.1.7) established by CDC on December 29, 2020 (Additional Table S7). We measured the levels of the fourteen miRNAs detected in the patient's plasma (Additional Table S6a) in the extracellular vesicles (EVs) secreted into the supernatants by the two infected lung epithelial cell lines. The SARS-CoV-2 Washington (USA-WA1/2020) infection induced an enrichment of hsa-miR-92b-3p and hsa-miR-93-5p in the secreted EVs compared with mock infection in two independent experiments, R1 and R2. Conversely, the infection with the variant SARS-CoV-2 UK (Alpha/B.1.1.7) had heterogeneous effects (Fig. 4). A heterogeneous effect was also measured for the other seven miRNAs (Additional Figure S5). The remaining five hsa-miR-150-3p, hsa-miR-150-5p, hsa-miR-182-5p, hsa-miR-486-5p, and hsa-miR-638 were not detected in any of the secreted EVs (Additional Table S6c).

We can conclude that the infection of lung epithelial cells by SARS-CoV-2 Washington (USA-WA1/2020) can be associated with a general modulation of miRNA levels measured in the secreted EVs.

Survival model for COVID-19-related death in cancer patients

We used the 10 miRNAs (Additional Table S6A) measured in plasma samples of both 2020 and 2021 cohorts collected at the time of the first COVID-19 positive test and four demographical features to evaluate if plasma levels of miRNAs could predict the time to death in patients with COVID-19. We tested 151 COVID-19-positive cancer patients treated at UT-MDACC during 2020 and 2021. Patients were randomly split into 106 (70%) individuals for the training set (with 16 deaths related to COVID-19 and 19 from other causes) and the remaining 45 (30%) individuals for the testing set (with four deaths related with COVID-19 and six from other causes). Time to event was defined as the interval between the first COVID-19

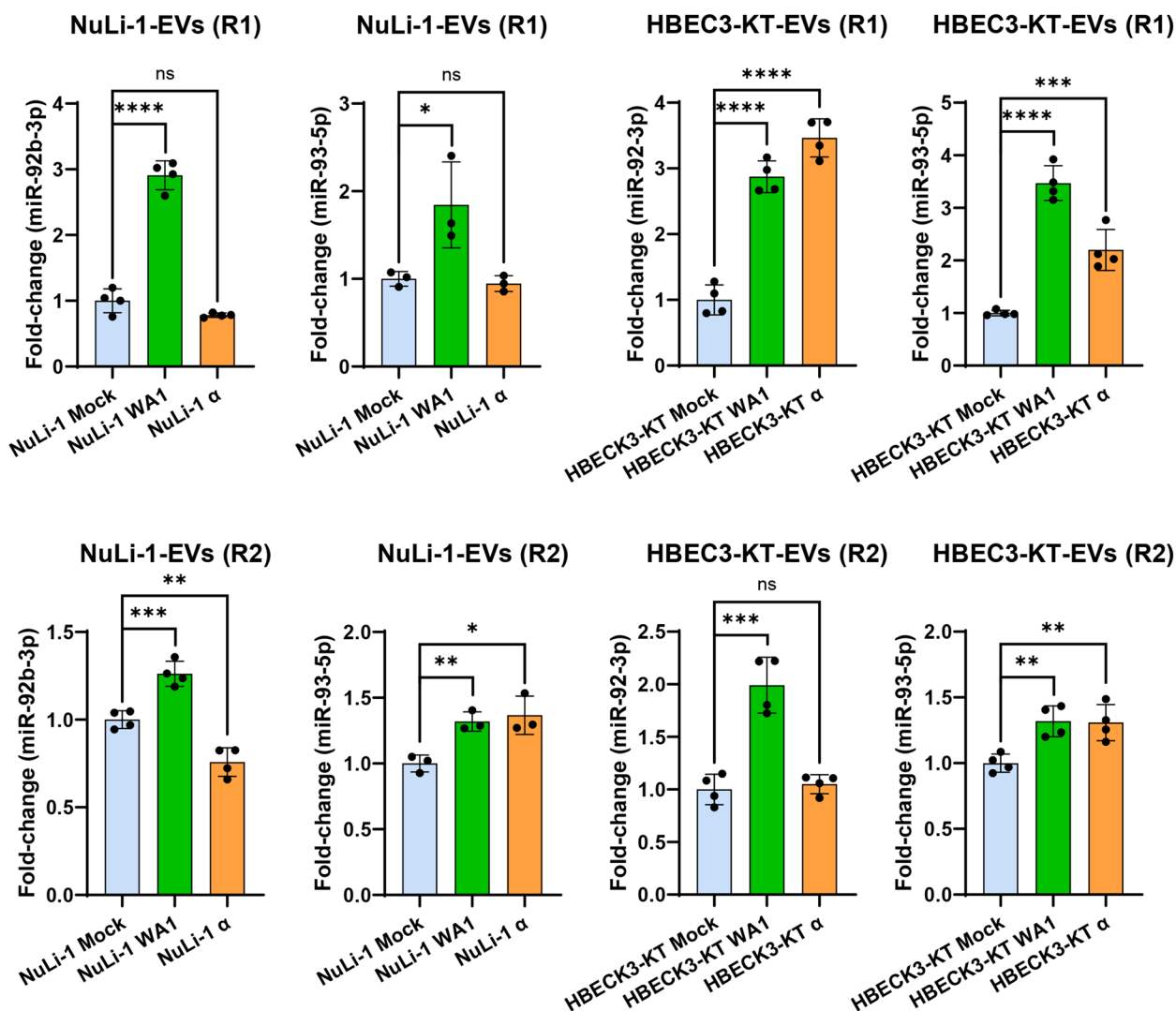


Fig. 4 Effect of SARS-CoV-2 infection on miRNA expression levels in the EVs secreted from normal bronchus epithelial cells. Levels of hsa-miR-92-3p and hsa-miR-93-5p were significantly enriched in the EVs secreted from NuLi-1 and HBECK3-KT cells after the infection with SARS-CoV-2 Washington (USA-WA1/2020). A heterogeneous effect was measured after infection with the variant SARS-CoV-2 UK (Alpha/B.1.1.7) (Unpaired t-test. *P* value summary: * < 0.05; ** < 0.01; *** < 0.001; **** < 0.0001; ns not significant)

positive test and death or the last follow-up time. In this study, deaths related to other causes precluded COVID-19-related death. Therefore, the analysis considered alternative causes of death as competing risk events.

In the training set, the plasma levels of hsa-miR-93-5p and hsa-miR-150-5p showed significant hazard ratios both in the sub-distributional hazard model [HR:0.31 (95% CI: 0.11–0.85); *P*=0.023] and HR:0.30 (95% CI: 0.11–0.83); *P*=0.020] and in cause-specific cox model [HR:0.31 (95% CI: 0.11–0.85); *P*=0.022 and HR:0.30 (95% CI: 0.11–0.82); *P*=0.019] for hsa-miR-93-5p and hsa-miR-150-5p, respectively (Additional Table S8). No significant associations were

observed in the non-COVID-19-related death cases (Additional Table S8). Patients were further stratified into low vs. high levels of the two miRNAs mentioned above based on median cut points. Their cumulative incidence plots yielded a statistically significant difference in COVID-19-related death (*P*=0.016 for hsa-miR-150-5p and *P*=0.014 for hsa-miR-93-5p (Fig. 5A and B). The probability of COVID-19-related death in 15 months for the low hsa-miR-150-5p group is found to be 20%, whereas it is observed to be around 7% in the high hsa-miR-150-5p group. However, the probability of non-COVID-19-related death is similar for low and high hsa-miR-150-5p groups (14% vs. 18%). Similar

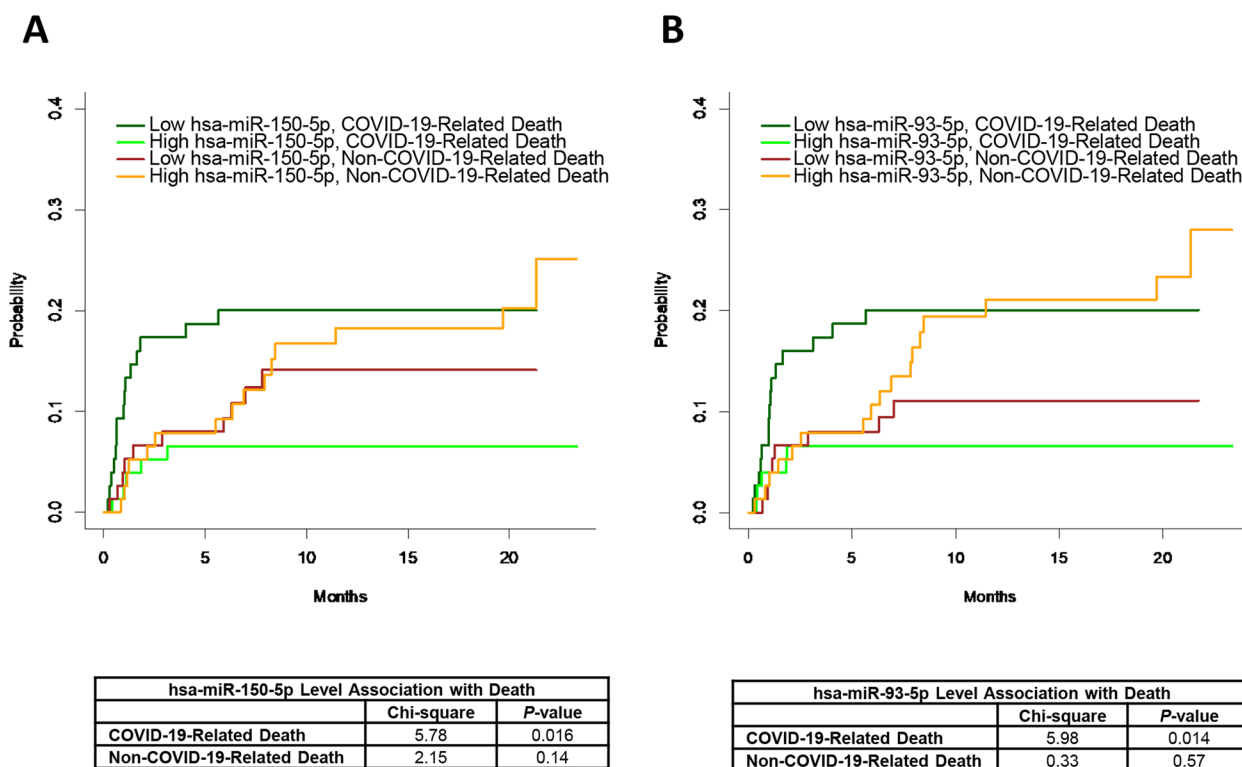


Fig. 5 Increased risk of COVID-19-related death for higher levels of hsa-miR-150-5p and hsa-miR-93-5p. **A** The probability of COVID-19-related and non-COVID-19-related death overtime stratified by high/low plasma levels of hsa-miR-150-5p; **B** The probability of COVID-19-related and non-COVID-19-related death overtime stratified by high/low plasma levels of hsa-miR-93-5p

findings were observed for hsa-miR-93-5p with a 20% vs. 7% probability of COVID-19-related death in low and high groups. Non-COVID-19-related death had 11% vs 21% probability in low and high groups. The number of patients at risk for each group is reported in the Additional Table S9.

A Cox Proportional Hazard model consisting of age, the plasma level of hsa-miR-150-5p and hsa-miR-93-5p developed on training group yielded concordance c-indexes of 78.2% and 74.3% with standard errors of 0.062 and 0.108 in training and testing sets, respectively. The AUC at each time point is consistently greater than 70% in training and testing groups (Additional Figure S6A). The estimated Cause-Specific Hazard model for COVID-19-related death had respective HR of 1.08, 6.29×10^{-13} , and 1.27×10^{-6} for age, hsa-miR-150-5p, and hsa-miR-93-5p, respectively (Additional Table S10). The results indicate that older age, lower plasma levels of hsa-miR-150-5p, and lower hsa-miR-93-5p are associated with higher COVID-19-related death risk. Our survival model shows excellent predictive power using the current internal validation mechanism. We further stratified patients into high versus low groups by median value and evaluated their survival performance for hsa-miR-150-5p and hsa-miR-93-5p. Our results indicate that low levels of both miRNAs are significantly associated with an increased risk of

COVID-19-related death (Fig. 5A, B and Additional Figure S6B).

Discussion

The data of our analysis indicate that some miRNAs located in regions in proximity to the SNPs associated with the severity and susceptibility of COVID-19 (CORSAIR) may be related to COVID-19 clinical outcomes of patients with cancer. Some pieces of evidence support this assumption. A remarkable number of miRNAs are located in CORSAIR. Among the 157 CORSAIR miRNAs, 29 miRNAs are co-expressed in both immune cells and normal lung epithelial cells, and at least three miRNAs (maximum 13) share the same confirmed target gene (Additional Table S11) based on miRTarbase [46]. Notably, among the 1678 identified target genes, 935 are proved to be targets of three combined miRNAs (minimum), five genes are targets of 10 combined miRNAs, and one gene is the target of 13 combined miRNAs (maximum). The convergence of multiple miRNAs on specific target genes is remarkable. Some of the top-ranked target genes are associated with COVID-19. Elevated amyloid beta precursor protein (APP)

was proposed to be involved in long-term neurological manifestations of COVID-19 disease [47], and patients with COVID-19-associated neurological syndromes exhibited impaired amyloid processing [48]. DICER1 is a ribonuclease required to produce the active small RNAs that repress gene expression. An isoform lacking exons 7 and 8 named antiviral Dicer (aviD) also acts as a potent antiviral agent with activity against RNA viruses, including the Zika and SARS-CoV-2 viruses [49]. LARP1, an essential effector protein in the mTOR pathway, may contribute to preferential translation of 5' terminal oligo-pyrimidine transcripts in response to the SARS-CoV-2 and relies on a nonstructural protein, Nsp1 expression involved in shutting down host translation [50]. LARP1 may have an antiviral function, as the gene depletion resulted in a substantial upregulation of SARS-CoV-2 RNA [51]. The signaling pathways of the targets of 29 co-expressed CORSAIR miRNAs (Additional Table S11) identified several pathways in the top 50 that are related to viral infections, including "Human cytomegalovirus infection" ($P=4.00305E-11$), "Human T-cell leukemia virus one infection" ($P=4.70875E-11$), "Kaposi sarcoma-associated herpesvirus infection" ($P=2.3361E-08$), "Human papillomavirus infection" ($P=5.81876E-08$), as well as "Immune System" ($P=1.98919E-08$) (Additional Table S12). We found the TGF-beta-signaling pathway on the top of the Hallmark pathways regulated by the four CORSAIR miRNAs highly expressed in immune cells, with the TGF-beta-signaling pathway playing an important role (inhibitory effects) in regulating T cell activation and differentiation [52, 53]. On the other hand, the top Hallmark pathway regulated by the 139 non-CORSAIR miRNAs highly expressed in immune cells was TNF-alpha signaling via NF-kB, which is involved in regulating inflammatory responses [54] (Additional Table S4a, 4b, 4c, 4d, 4e). Finally, some of the SNPs we studied are located in proximity of candidate Cis-Regulatory Elements (cCREs), such as promoter-like (PLS), proximal enhance-like (pELS), and distal enhancer-like (dELS) signatures, based on UCSC Genome Browser Genome on Human (GRCh38/hg38). Two examples are reported for rs11541192 and rs4801778 (Additional Figure S7).

Cancer patients are at high risk for aggressive COVID-19 evolution and adverse clinical outcomes. It has been previously reported that circulating miRNAs have the potential to work as biomarkers for COVID-19 and the severity of the disease. In particular, a signature of three miRNAs (miR-148a-3p, miR-451a, and miR-486-5p) could distinguish between patients admitted to the intensive care unit (ICU) and ward patients [AUC (95% CI)=0.89 (0.81–0.97)]. Among critically ill patients, a signature based on two miRNAs

(miR-192-5p and miR-323a-3p) differentiated ICU non-survivors from survivors [AUC (95% CI)=0.80 (0.64–0.96)] [55]. In another study, the serum levels of the miR-92a-2-5p were negatively correlated with degrees of adverse reactions after COVID-19 vaccination, whereas miR-148a levels were associated with specific antibody titers [56]. Another study detected significant changes in the levels of circulating miR-150-5p, miR-375, miR-122-5p, miR-494-3p, miR-3197, miR-4690-5p, miR-1915-3p, and miR-3652 in the plasma of COVID-19 patients compared with healthy controls. Furthermore, a sharp decline in the miR-150-5p plasma levels in COVID-19 patients could enhance SARS-CoV-2 infection. MiR-150-5p regulates the SARS-CoV-2 encoded non-structural protein 10 (*nsp10*) gene, essential for viral replication and in evading host immune response [57–59]. The above studies were conducted on non-cancer patients.

Based on this evidence, we evaluated the levels of miRNAs located in CORSAIR in the plasma of cancer patients and correlated them with their clinical outcomes. We found that low plasma levels of hsa-miR-150-5p were associated with higher COVID-19-related death. Because we previously showed that low plasma levels of hsa-miR-150-5p were associated with bacterial sepsis [35], we hypothesized that there might be potential similarities between the two types of infections during the acute phase, even though they are two different types of infectious diseases (SARS-CoV-2 and bacterial infection) [60, 61]. We saw a similar association with hsa-miR-93-5p, a sepsis-related miRNA. The similarity could consist of the cytokine storm syndrome. However, the time course (hours/few days vs. several days) and the immune response types (bacterial vs. viral) may differ between sepsis and COVID-19. We investigated if the plasma levels of hsa-miR-150-5p and hsa-miR-93-5p could derive from immune cells. We found significantly increasing levels of these two miRNAs in the supernatants of PBMC at three and six days after activation with TLR7/8 agonist (R848) and antigen-independent T cell activator (conc A). The increased levels in the supernatant demonstrated that the activation of immune cells (monocytes/macrophages, dendritic cells, and T cells) was associated with a higher secretion of hsa-miR-150-5p and hsa-miR-93-5p. We also measured this increase in healthy individuals' plasma after receiving the second dose of the Pfizer-BioNTech COVID-19 vaccine. A similar increase was measured for hsa-miR-92b-3p. Therefore, the high plasma levels of hsa-miR-150-5p, hsa-miR-93-5p, and hsa-miR-92b-3p in vaccinated healthy individuals may result from an effective immune cell activation and the anti-SARS-CoV-2 response. Conversely, the low plasma

levels of hsa-miR-150-5p and hsa-miR-93-5p in cancer patients infected by SARS-CoV-2 and who died from COVID-19-related causes may result from an ineffective immune cell activation and response to viral infection responsible for the adverse clinical outcomes [62]. On the other hand, the decreased plasma levels of hsa-miR-92b-3p in cancer patients that became negative for the SARS-CoV-2 test may reflect an off-switch process of the immune responses (resolution) during the recovery from COVID-19.

We previously showed that low levels of hsa-miR-150-5p were associated with high levels of its targets IL-10 and IL-18 [35], which can promote Th2 cell-mediated immune response. IL-10, a Th2 cell cytokine and highly expressed by Treg cells (immunosuppressive) [63], inhibits the secretion of IL-12 and IFN- γ and accordingly blocks the polarization of Th0 cells into Th1 cells [64], which are a central player in the anti-viral immune response [60, 63]. Furthermore, in absence of IL-12, IL-18 facilitates Th2 cell-mediated responses through IL-3, IL-9, and IL-13 [65]. Th1 cell-mediated immune response is associated with the resolution of COVID-19 and good prognosis [66]. In contrast, an overreactive Th2-cell-mediated response is associated with poor prognosis [67, 68]. Therefore, low plasma levels of hsa-miR-150-5p could be associated with an increased risk of poor prognosis because of sustained Th2 cell-mediated response, with high levels of IL-10 [69, 70] and IL-18 associated with poor prognosis in COVID-19 [71–74]. Furthermore, Th2 cell-mediated response could hinder SARS-CoV-2 infection resolution (prolonged infection), determining an additional effort of the immune system to clear the infection associated with high levels of pro-inflammatory cytokines (IFN- α , IFN- γ , IL-1 β , IL-6, IL-12, IL-15, IL-18, IL-33, IP-10) [67, 75].

Dysregulated host immune response is a characteristic of bacterial sepsis and, similar to COVID-19, aberrant levels of cytokines, hyperinflammatory “cytokine storm” response, and altered balance of T cell co-stimulatory and co-inhibitory signaling occur [76]. Increasing evidence proposes a potential role of host Th17 inflammatory responses in contributing to severe COVID-19 and unfavorable prognosis [77–80], in which IL-1 β , IL-6, IL-17, TNF- α , GM-CSF, and IFN- γ are involved in Th17-related responses [81] associated with ARDS leading to pulmonary edema, lung failure, and liver, heart, and kidney damage [3, 80]. Significantly, hsa-miR-93-5p regulates Th17 cell differentiation by targeting STAT3 [82, 83]. Furthermore, it was reported that Th17 cells enhanced viral persistence and inhibited T cell cytotoxicity via IL-17, resulting in chronic inflammatory disease [84]. Therefore, low levels of hsa-miR-93-5p might be associated with a Th-17

cell-mediated response to SARS-CoV-2 infection and be responsible for severe COVID-19. It might be hypothesized that low levels of both hsa-miR-150-5p and hsa-miR-93-5p in patients with poor prognosis are associated with a reduced ability to clear the SARS-CoV-2 infection due to a Th2 cell-skewed immune response and a Th-17 cell-mediated pro-inflammatory response.

It was found that hsa-miR-92b-3p, a potent regulator of the mTOR signaling pathways, was induced by hypoxia in pulmonary artery smooth muscle cells (PASMCs) and induced their proliferation by targeting TSC1, a negative regulator in the mTOR signaling [85]. Therefore, it is possible that during SARS-CoV-2 infection, high levels of hsa-miR-92b-3p may be induced in the lung tissue and promote PASMC proliferation in response to tissue damage during COVID-19. In addition, it was found that in primary normal bronchial epithelial cells (NHBE) treated with IL-13, a type 2 T helper (Th2) cell cytokine used to induce an asthma-like phenotype of the airway epithelium, hsa-miR-92b-3p was the most downregulated miRNAs measured in secreted EVs in response to IL-13 [86]. Because recovering patients who became COVID-19 negative had a concomitant reduction of hsa-miR-92b-3p plasma levels (Fig. 2B), this decrease may result from the counterbalancing Th2-mediated response reflecting the declining of the anti-viral Th1-mediated immune responses during the recovery phase from the disease [63] and reflect the non-infected status of the human airway epithelial cells. Therefore, the variation of hsa-miR-92b-3p plasma levels may correlate with the infection and stress status of the human airway epithelium, and the decreased plasma levels of hsa-miR-92b-3p that were measured when patients became SARS-CoV-2 negative may reflect the recovery process of the infected lung tissue. Because both NuLi-1 and HBEC3-KT cells did not express and secrete detectable levels of hsa-miR-150-5p after mock and SARS-CoV-2 infection, whereas increased levels of hsa-miR-150-5p were measured in the supernatants of activated PBMC ($d=6$) and after Pfizer/BioNTech vaccination, the variation of levels of hsa-miR-150-5p in the plasma of cancer patients may primarily result from an effective immune response and not from infected lung epithelial cells.

Conclusions

In conclusion, our study presents a novel approach to identifying miRNAs as predictor biomarkers of disease aggressivity and effective immune responses to SARS-CoV-2 in cancer patients based on their location at specific COVID-19 risk-associated genomic regions,

CORSAIR, identified by genome-wide association studies. Besides miRNAs, other classes of non-coding RNAs, such as long non-coding RNAs (lncRNAs), located in the CORSAIR, could be potentially investigated. We acknowledge that some weaknesses are present in our study. More comprehensive and in-depth studies on the regulatory associations between CORSAIR miRNAs and COVID-19-related SNPs are required to better evaluate their functional mechanisms in COVID-19. Furthermore, additional studies are necessary to dissect the individual cell contribution to the miRNAs measured in the plasma, and time course analyses are essential to evaluate the variation of each miRNA across the different stages of COVID-19. Finally, an in-depth analysis using blood samples from specific and homogenous populations of cancer patients (e.g., same cancer types) is required.

Finally, we believe that a similar approach used in this study can potentially be used to identify patients at risk for poor clinical outcomes in viral infections other than COVID-19, for example, flu (influenza viruses), cytomegalovirus, cold (rhinoviruses, parainfluenza, and seasonal coronaviruses) that can cause severe complications (e.g., pneumonia) and negatively impact the prognosis of immunocompromised and fragile patients, such as cancer patients.

Abbreviations

ARDS	Acute respiratory distress syndrome
AUC	Area under the curve
CORSAIR	COVid-19 RiSk Associated genomic Regions
COVID-19	Coronavirus disease 2019
CSH	Cause-Specific Hazard
EVs	Extracellular vesicles
GLM	Generalized linear model
GWAS	Genome-wide association studies
MFP	Multivariate fractional polynomial
miRNAs	MicroRNAs
ROC	Receiver Operating Characteristic
SARS-CoV-2	Severe acute respiratory syndrome coronavirus 2
SNPs	Single nucleotide polymorphisms

Supplementary Information

The online version contains supplementary material available at <https://doi.org/10.1186/s12943-024-02094-9>.

Supplementary Material 1: Additional Figure S1. Association of genomic location between SNPs and non-coding ultra-conserved elements (ncUCEs) and miRNAs. A) Boxplots for the regions with and without SNPs versus the number of ncUCEs; B) Boxplots for the regions with and without SNPs versus the expected number of miRNAs by chromosome number. Additional Figure S2. The reproducibility of RT-qPCR results in two independent experimental replicates. The RT-qPCR amplification (Ct values) showed high levels of reproducibility in two independent experimental replicates, confirming the excellent quality of the RNA samples and technical procedures (Spearman Correlation for two biological replicate data for hsa-miR-150-5p and hsa-miR-93-5p). Additional Figure S3. Levels of miRNAs in activated peripheral blood mononuclear cells (PBMC), their supernatants, and in serum samples of Pfizer-BioNTech vaccinated healthy individuals. A) Variation of the expression levels of the remaining eleven

selected miRNAs in PBMC at six days after activation with TLR-7/8 agonist (α TLR7/8) and T cell mitogen concanavalin A (conc A), compared with unstimulated PBMC; B) Variation of the expression levels of the remaining eleven selected miRNAs in the supernatants of PBMC at three and six days after activation with α TLR7/8 and conc A, compared with supernatant of unstimulated PBMC; C) Variation of hsa-miR-92b-3p, hsa-miR-150-5p, and hsa-miR-93-5p in the pair-matched serum samples of healthy individuals ($n = 23$) at one, six, and nine months after the administration of the second dose of the Pfizer-BioNTech vaccine (Wilcoxon test); D) Variation of the SARS-CoV-2 anti-spike (S) protein IgG in the serum samples of healthy individuals at different times after the administration of the second dose of the Pfizer-BioNTech vaccine (In A and B, Unpaired t-test. *P* value summary: * < 0.05; ** < 0.01; *** < 0.001; **** < 0.0001; ns not significant). Additional Figure S4. Gene set enrichment analysis (GSEA). Hallmark pathway analysis for A) CORSAIR and B) non-CORSAIR miRNAs with expression higher than one standard deviation (4 CORSAIR and 139 non-CORSAIR miRNAs). Additional Figure S5. Effect of SARS-CoV-2 infection on miRNA expression levels in the EVs secreted from normal bronchus epithelial cells. Variation of the expression levels of the remaining seven selected miRNAs in the secreted EVs from NuLi-1 and HBEC3-KT normal lung epithelial cells after infection with SARS-CoV-2 Washington (USA-WA1/2020) and SARS-CoV-2 UK (Alpha B.1.1.7) (Unpaired t-test. *P* value summary: * < 0.05; ** < 0.01; *** < 0.001; **** < 0.0001). Additional Figure S6. The probability of COVID-19-related and non-COVID-19-related death across time stratified by high/low expression levels of hsa-miR-150-5p and hsa-miR-93-5p combinations. A) The AUC is consistently greater than 70% in both training and testing groups across time; B) The combination of low levels of both hsa-miR-150-5p and hsa-miR-93-5p were associated with increased risk of COVID-19-related death. Additional Figure S7. Genomic localization of SNPs associated with the risk of aggressive COVID-19. The SNPs we studied are generally located in the proximity of candidate Cis-Regulatory Elements (cCREs), such as promoter-like (PLS), proximal enhance-like (pELS), and distal enhancer-like (dELS) signatures, based on UCSC Genome Browser Genome on Human (GRCh38/hg38). In addition, we reported an example of two SNPs: (A) rs11541192 and (B) rs4801778.

Supplementary Material 2. Additional Tables.

Supplementary Material 3. Supplementary Methods.

Acknowledgements

Dr. Calin is the Felix L. Haas Endowed Professor in Basic Science. Work in G.A.C.'s laboratory is supported by NCI grant 1R01CA222007-01A1, NIDCR grant R01DE032018, DoD CDRMP Idea Award BC200208P1 (W81XWH-21-1-0030), Team DOD grant in Gastric Cancer CA200990P2 (W81XWH-21-1-0715), DoD Idea Award PC230419 (HT9425-24-1-0052), the 2019 Faculty Achievement Award, CLL Global Research Foundation 2019 grant, CLL Global Research Foundation 2020 grant, CLL Global Research Foundation 2022 grant, CLL Global Research Foundation 2024 grant, The G. Harold & Leila Y. Mathers Foundation, two grants from Torrey Coast Foundation, an Institutional Research Grant 2024, a Development Grant associated with the Brain SPORE 2P50CA127001, an Institutional Bridge Funding grant 2023, and the Ben and Catherine Ivy Foundation grant. Dr. Ziyi Li (ZL) is partly supported by the NCI grant R03CA270725. Dr. Kim-Anh Do (KAD) was partially supported by a Cancer Center Support Grant NCI Grant P30 CA016672, NIH grants UL1TR003167, 5R01GM122775, the prostate cancer SPORE P50 CA140388, CPRIT grant RP160693, and the Moon Shots funding at MD Anderson Cancer Center.

Authors' contributions

GC and SA conceived and designed the research study. MS and MW conducted most of the experiments. SA and FD acquired and analyzed data and prepared figures and tables. JQ, PR, and MC collected data and prepared tables. SC collected clinical data and prepared the clinical table. IW and EB provided and collected plasma samples. SA, FD, KAD, ZL and GC analyzed data. IM provided SARS-CoV-2 infected cell line samples. LA and TRO provided and collected the serum samples from healthy individuals. LA performed the serologic tests, and TRO provided the laboratory test results of the collected sera and data regarding healthy individuals. SA and GC wrote the manuscript. GC obtained funds for the project.

Availability of data and materials

All data generated or analyzed during this study are included in this published article and its Additional information files.

Declarations**Competing interests**

The authors declare no competing interests.

Author details

¹Department of Translational Molecular Pathology, The University of Texas MD Anderson Cancer Center, Houston, USA. ²Department of Hematopoietic Biology & Malignancy, The University of Texas MD Anderson Cancer Center, Houston, USA. ³Department of Hemopathology, The University of Texas MD Anderson Cancer Center, Houston, USA. ⁴Department of Microbiology, Immunology and Cell Biology, West Virginia University Cancer Institute, Morgantown, USA. ⁵Department of Pathology, The University of Texas MD Anderson Cancer Center, Houston, USA. ⁶Department of Biostatistics, The University of Texas MD Anderson Cancer Center, Houston, USA. ⁷Clinical Laboratory, Municipal Clinical Emergency Hospital, Timisoara, Romania. ⁸Department of Infectious Diseases, Center for Diagnosis and Study of Parasitic Diseases, Victor Babes University of Medicine and Pharmacy, Timisoara, Romania. ⁹The Non-coding RNA Center, The University of Texas MD Anderson Cancer Center, Houston, USA.

Received: 16 August 2023 Accepted: 18 August 2024

Published online: 21 October 2024

References

- Dorward DA, Russell CD, Um IH, Elshani M, Armstrong SD, Penrice-Randal R, Millar T, Lerpiniere CEB, Tagliavini G, Hartley CS, et al. Tissue-Specific Immunopathology in Fatal COVID-19. *Am J Respir Crit Care Med*. 2021;203:192–201.
- Wang D, Hu B, Hu C, Zhu F, Liu X, Zhang J, Wang B, Xiang H, Cheng Z, Xiong Y, et al. Clinical Characteristics of 138 Hospitalized Patients With 2019 Novel Coronavirus-Infected Pneumonia in Wuhan. *China JAMA*. 2020;323:1061–9.
- Huang C, Wang Y, Li X, Ren L, Zhao J, Hu Y, Zhang L, Fan G, Xu J, Gu X, et al. Clinical features of patients infected with 2019 novel coronavirus in Wuhan. *China Lancet*. 2020;395:497–506.
- Zhang B, Zhou X, Qiu Y, Song Y, Feng F, Feng J, Song Q, Jia Q, Wang J. Clinical characteristics of 82 cases of death from COVID-19. *PLoS ONE*. 2020;15: e0235458.
- Tay MZ, Poh CM, Renia L, MacAry PA, Ng LFP. The trinity of COVID-19: immunity, inflammation and intervention. *Nat Rev Immunol*. 2020;20:363–74.
- Goldman JD, Gonzalez MA, Rührich MM, Sharon E, von Lilienfeld-Toal M. COVID-19 and Cancer: Special Considerations for Patients Receiving Immunotherapy and Immunosuppressive Cancer Therapies. *Am Soc Clin Oncol Educ Book*. 2022;42:1–13.
- Nakanishi T, Pigazzini S, Degenhardt F, Cordioli M, Butler-Laporte G, Maya-Miles D, Bujanda L, Bouysran Y, Niemi ME, Palom A, et al. Age-dependent impact of the major common genetic risk factor for COVID-19 on severity and mortality. *J Clin Invest*. 2021;131(23):e152386.
- Pairo-Castineira E, Clohisey S, Klaric L, Bretherick AD, Rawlik K, Pasko D, Walker S, Parkinson N, Fourman MH, Russell CD, et al. Genetic mechanisms of critical illness in COVID-19. *Nature*. 2021;591:92–8.
- Severe Covid GG, Ellinghaus D, Degenhardt F, Bujanda L, Buti M, Alballos A, Invernizzi P, Fernandez J, Prati D, Baselli G, et al. Genomewide Association Study of Severe Covid-19 with Respiratory Failure. *N Engl J Med*. 2020;383:1522–34.
- Anastassopoulou C, Gkizarioti Z, Patrinos GP, Tsakris A. Human genetic factors associated with susceptibility to SARS-CoV-2 infection and COVID-19 disease severity. *Hum Genomics*. 2020;14:40.
- Forbester JL, Humphreys IR. Genetic influences on viral-induced cytokine responses in the lung. *Mucosal Immunol*. 2021;14:14–25.
- Calin GA, Sevignani C, Dumitru CD, Hyslop T, Noch E, Yendamuri S, Shimizu M, Rattan S, Bullrich F, Negrini M, Croce CM. Human microRNA genes are frequently located at fragile sites and genomic regions involved in cancers. *Proc Natl Acad Sci U S A*. 2004;101:2999–3004.
- Giza DE, Fuentes-Mattei E, Bullock MD, Tudor S, Goblirsch MJ, Fabbri M, Lupu F, Yeung SJ, Vasilescu C, Calin GA. Cellular and viral microRNAs in sepsis: mechanisms of action and clinical applications. *Cell Death Differ*. 2016;23:1906–18.
- Mehta A, Baltimore D. MicroRNAs as regulatory elements in immune system logic. *Nat Rev Immunol*. 2016;16:279–94.
- Virga F, Cappellesso F, Stijlemans B, Henze AT, Trotta R, Van Audenaerde J, Mirchandani AS, Sanchez-Garcia MA, Vandewalle J, Orso F, et al. Macrophage miR-210 induction and metabolic reprogramming in response to pathogen interaction boost life-threatening inflammation. *Sci Adv*. 2021;7(19):eabf0466.
- Mittelbrunn M, Gutierrez-Vazquez C, Villarroya-Beltri C, Gonzalez S, Sanchez-Cabo F, Gonzalez MA, Bernad A, Sanchez-Madrid F. Unidirectional transfer of microRNA-loaded exosomes from T cells to antigen-presenting cells. *Nat Commun*. 2011;2:282.
- Okoye IS, Coomes SM, Pelly VS, Czieso S, Papayannopoulos V, Tolmachova T, Seabra MC, Wilson MS. MicroRNA-Containing T-Regulatory-Cell-Derived Exosomes Suppress Pathogenic T Helper 1 Cells. *Immunity*. 2014;41:503.
- Blanchard N, Lankar D, Faure F, Regnault A, Dumont C, Raposo G, Hivroz C. TCR activation of human T cells induces the production of exosomes bearing the TCR/CD3/zeta complex. *J Immunol*. 2002;168:3235–41.
- Yang M, Chen J, Su F, Yu B, Su F, Lin L, Liu Y, Huang JD, Song E. Microvesicles secreted by macrophages shuttle invasion-potentiating microRNAs into breast cancer cells. *Mol Cancer*. 2011;10:117.
- Alexander M, Hu R, Runtsch MC, Kagele DA, Mosbrugger TL, Tolmachova T, Seabra MC, Round JL, Ward DM, O'Connell RM. Exosome-delivered microRNAs modulate the inflammatory response to endotoxin. *Nat Commun*. 2015;6:7321.
- Anfossi S, Giordano A, Gao H, Cohen EN, Tin S, Wu Q, Garza RJ, Debeb BG, Alvarez RH, Valero V, et al. High serum miR-19a levels are associated with inflammatory breast cancer and are predictive of favorable clinical outcome in patients with metastatic HER2+ inflammatory breast cancer. *PLoS ONE*. 2014;9: e83113.
- Anfossi S, Babayan A, Pantel K, Calin GA. Clinical utility of circulating non-coding RNAs - an update. *Nat Rev Clin Oncol*. 2018;15:541–63.
- Olariu TR, Ursoniu S, Marinicu I, Lupu M. Dynamics of Antibody Response to BNT162b2 mRNA COVID-19 Vaccine: A 7-Month Follow-Up Study. *Medicina (Kaunas)*. 2021;57(12):1330.
- Polack FP, Thomas SJ, Kitchin N, Absalon J, Gurtman A, Lockhart S, Perez JL, Perez Marc G, Moreira ED, Zerbini C, et al. Safety and Efficacy of the BNT162b2 mRNA Covid-19 Vaccine. *N Engl J Med*. 2020;383:2603–15.
- EUA Authorized Serology Test Performance. <https://www.fda.gov/medical-devices/covid-19-emergency-use-authorizations-medical-devices/eua-authorized-serology-test-performance>.
- Patrick Royston WS. Multivariable Model - Building: A Pragmatic Approach to Regression Analysis based on Fractional Polynomials for Modelling Continuous Variables. Hoboken: Wiley; 2008.
- Fine JP, Gray RJ. A proportional hazards model for the subdistribution of a competing risk. *J Am Stat Assoc*. 1999;94:496–509.
- Gray RJ. A Class of K-Sample Tests for Comparing the Cumulative Incidence of a Competing Risk. *Ann Stat*. 1988;16:1141–54.
- Blobel GA, Higgs DR, Mitchell JA, Notani D, Young RA. Testing the super-enhancer concept. *Nat Rev Genet*. 2021;22:749–55.
- Grimwood J, Gordon LA, Olsen A, Terry A, Schmutz J, Lamerdin J, Hellsten U, Goodstein D, Couronne O, Tran-Gyamfi M, et al. The DNA sequence and biology of human chromosome 19. *Nature*. 2004;428:529–35.
- Flor I, Bullerdiek J. The dark side of a success story: microRNAs of the C19MC cluster in human tumours. *J Pathol*. 2012;227:270–4.
- Stephen S, Pheasant M, Makunin IV, Mattick JS. Large-scale appearance of ultraconserved elements in tetrapod genomes and slowdown of the molecular clock. *Mol Biol Evol*. 2008;25:402–8.
- Leidinger P, Backes C, Meder B, Meese E, Keller A. The human miRNA repertoire of different blood compounds. *BMC Genomics*. 2014;15:474.
- Initiative C-HG. Mapping the human genetic architecture of COVID-19. *Nature*. 2021;600:472–7.
- Vasilescu C, Rossi S, Shimizu M, Tudor S, Veronese A, Ferracin M, Nicoloso MS, Barbarotto E, Popa M, Stanculea O, et al. MicroRNA fingerprints identify miR-150 as a plasma prognostic marker in patients with sepsis. *PLoS ONE*. 2009;4:e7405.
- Galvan-Pena S, Leon J, Chowdhary K, Michelson DA, Vijaykumar B, Yang L, Magnuson AM, Chen F, Manickas-Hill Z, Piechocka-Trocha A, et al.

- Profound Treg perturbations correlate with COVID-19 severity. *Proc Natl Acad Sci U S A*. 2021;118(37):e2111315118.
37. Lucas C, Wong P, Klein J, Castro TBR, Silva J, Sundaram M, Ellingson MK, Mao T, Oh JE, Israelow B, et al. Longitudinal analyses reveal immunological misfiring in severe COVID-19. *Nature*. 2020;584:463–9.
 38. Sohn KM, Lee SG, Kim HJ, Cheon S, Jeong H, Lee J, Kim IS, Silwal P, Kim YJ, Paik S, et al. COVID-19 Patients Upregulate Toll-like Receptor 4-mediated Inflammatory Signaling That Mimics Bacterial Sepsis. *J Korean Med Sci*. 2020;35: e343.
 39. Bhaskar S, Sinha A, Banach M, Mittoo S, Weissert R, Kass JS, Rajagopal S, Pai AR, Kutty S. Cytokine Storm in COVID-19-Immunopathological Mechanisms, Clinical Considerations, and Therapeutic Approaches: The REPROGRAM Consortium Position Paper. *Front Immunol*. 2020;11:1648.
 40. Tudor S, Giza DE, Lin HY, Fabris L, Yoshiaki K, D'Abundo L, Toale KM, Shimizu M, Ferracin M, Challagundla KB, et al. Cellular and Kaposi's sarcoma-associated herpes virus microRNAs in sepsis and surgical trauma. *Cell Death Dis*. 2014;5: e1559.
 41. Dragomir MP, Fuentes-Mattei E, Winkle M, Okubo K, Bayraktar R, Knutsen E, Qdaisat A, Chen M, Li Y, Shimizu M, et al. Anti-miR-93–5p therapy prolongs sepsis survival by restoring the peripheral immune response. *J Clin Invest*. 2023;133(14):e158348.
 42. Di Felice G, Visci G, Teglia F, Angelini M, Boffetta P. Effect of cancer on outcome of COVID-19 patients: a systematic review and meta-analysis of studies of unvaccinated patients. *Elife*. 2022;11:e74634.
 43. Gutierrez-Vazquez C, Rodriguez-Galan A, Fernandez-Alfara M, Mittelbrunn M, Sanchez-Cabo F, Martinez-Herrera DJ, Ramirez-Huesca M, Pascual-Montano A, Sanchez-Madrid F. miRNA profiling during antigen-dependent T cell activation: A role for miR-132–3p. *Sci Rep*. 2017;7:3508.
 44. Rodriguez-Galan A, Dosal SG, Gomez MJ, Fernandez-Delgado I, Fernandez-Messina L, Sanchez-Cabo F, Sanchez-Madrid F. miRNA post-transcriptional modification dynamics in T cell activation. *iScience*. 2021;24:102530.
 45. Wahlgren J, Karlson Tde L, Glader P, Teleme E, Valadi H. Activated human T cells secrete exosomes that participate in IL-2 mediated immune response signaling. *PLoS ONE*. 2012;7: e49723.
 46. Huang HY, Lin YC, Li J, Huang KY, Shrestha S, Hong HC, Tang Y, Chen YG, Jin CN, Yu Y, et al. miRTarBase 2020: updates to the experimentally validated microRNA-target interaction database. *Nucleic Acids Res*. 2020;48:D148–54.
 47. Camacho RC, Alabed S, Zhou H, Chang SL. Network Meta-analysis on the Changes of Amyloid Precursor Protein Expression Following SARS-CoV-2 Infection. *J Neuroimmunol Pharmacol*. 2021;16:756–69.
 48. Ziff OJ, Ashton NJ, Mehta PR, Brown R, Athauda D, Heaney J, Heslegrave AJ, Benedet AL, Blennow K, Checkley AM, et al. Amyloid processing in COVID-19 associated neurological syndromes. *J Neurochem*. 2022;161(2):146–57.
 49. Poirier EZ, Buck MD, Chakravarty P, Carvalho J, Frederico B, Cardoso A, Healy L, Ulferts R, Beale R, Reis e Sousa C. An isoform of Dicer protects mammalian stem cells against multiple RNA viruses. *Science*. 2021;373:231–6.
 50. Rao S, Hoskins I, Tonn T, Garcia PD, Ozadam H, Sarinay Cenik E, Cenik C. Genes with 5' terminal oligopyrimidine tracts preferentially escape global suppression of translation by the SARS-CoV-2 Nsp1 protein. *RNA*. 2021;27:1025–45.
 51. Lee S, Lee YS, Choi Y, Son A, Park Y, Lee KM, Kim J, Kim JS, Kim VN. The SARS-CoV-2 RNA interactome. *Mol Cell*. 2021;81(2838–2850): e2836.
 52. Sanjabi S, Oh SA, Li MO. Regulation of the Immune Response by TGF-beta: From Conception to Autoimmunity and Infection. *Cold Spring Harb Perspect Biol*. 2017;9(6):a022236.
 53. Gorelik L, Flavell RA. Transforming growth factor-beta in T-cell biology. *Nat Rev Immunol*. 2002;2:46–53.
 54. Bradley JR. TNF-mediated inflammatory disease. *J Pathol*. 2008;214:149–60.
 55. de Gonzalo-Calvo D, Benitez ID, Pinilla L, Carratala A, Moncusi-Moix A, Gort-Paniello C, Molinero M, Gonzalez J, Torres G, Bernal M, et al. Circulating microRNA profiles predict the severity of COVID-19 in hospitalized patients. *Transl Res*. 2021;236:147–59.
 56. Miyashita Y, Yoshida T, Takagi Y, Tsukamoto H, Takashima K, Kouwaki T, Makino K, Fukushima S, Nakamura K, Oshiumi H. Circulating extracellular vesicle microRNAs associated with adverse reactions, proinflammatory cytokine, and antibody production after COVID-19 vaccination. *NPJ Vaccines*. 2022;7:16.
 57. Akula SM, Bolin P, Cook PP. Cellular miR-150-5p may have a crucial role to play in the biology of SARS-CoV-2 infection by regulating nsp10 gene. *RNA Biol*. 2022;19:1–11.
 58. Vithani N, Ward MD, Zimmerman MI, Novak B, Borowsky JH, Singh S, Bowman GR. SARS-CoV-2 Nsp16 activation mechanism and a cryptic pocket with pan-coronavirus antiviral potential. *Biophys J*. 2021;120:2880–9.
 59. Bouvet M, Lugari A, Posthuma CC, Zevenhoven JC, Bernard S, Betzi S, Imbert I, Canard B, Guillemot JC, Lecine P, et al. Coronavirus Nsp10, a critical co-factor for activation of multiple replicative enzymes. *J Biol Chem*. 2014;289:25783–96.
 60. Rouse BT, Sehrawat S. Immunity and immunopathology to viruses: what decides the outcome? *Nat Rev Immunol*. 2010;10:514–26.
 61. Giamarellos-Bourboulis EJ, Raftogiannis M. The immune response to severe bacterial infections: consequences for therapy. *Expert Rev Anti Infect Ther*. 2012;10:369–80.
 62. Goodyear CS, Patel A, Barnes E, Willicombe M, Siebert S, de Silva TI, Snowden JA, Lim SH, Bowden SJ, Billingham L, et al. Immunogenicity of third dose COVID-19 vaccine strategies in patients who are immunocompromised with suboptimal immunity following two doses (OCTAVE-DUO): an open-label, multicentre, randomised, controlled, phase 3 trial. *Lancet Rheumatol*. 2024;6:e339–51.
 63. Spellberg B, Edwards JE Jr. Type 1/Type 2 immunity in infectious diseases. *Clin Infect Dis*. 2001;32:76–102.
 64. Ito S, Ansari P, Sakatsume M, Dickensheets H, Vazquez N, Donnelly RP, Larner AC, Finbloom DS. Interleukin-10 inhibits expression of both interferon alpha- and interferon gamma- induced genes by suppressing tyrosine phosphorylation of STAT1. *Blood*. 1999;93:1456–63.
 65. Nakanishi K. Unique Action of Interleukin-18 on T Cells and Other Immune Cells. *Front Immunol*. 2018;9:763.
 66. Neidleman J, Luo X, Frouard J, Xie G, Gill G, Stein ES, McGregor M, Ma T, George AF, Kusters A, et al. SARS-CoV-2-Specific T Cells Exhibit Phenotypic Features of Helper Function, Lack of Terminal Differentiation, and High Proliferation Potential. *Cell Rep Med*. 2020;1: 100081.
 67. Gil-Etayo FJ, Suarez-Fernandez P, Cabrera-Marante O, Arroyo D, Garcinuno S, Naranjo L, Pleguezuelo DE, Allende LM, Mancebo E, Lalueza A, et al. T-Helper Cell Subset Response Is a Determining Factor in COVID-19 Progression. *Front Cell Infect Microbiol*. 2021;11: 624483.
 68. Roncati L, Nasillo V, Lusenti B, Riva G. Signals of T(H)2 immune response from COVID-19 patients requiring intensive care. *Ann Hematol*. 2020;99:1419–20.
 69. Han H, Ma Q, Li C, Liu R, Zhao L, Wang W, Zhang P, Liu X, Gao G, Liu F, et al. Profiling serum cytokines in COVID-19 patients reveals IL-6 and IL-10 are disease severity predictors. *Emerg Microbes Infect*. 2020;9:1123–30.
 70. Zhao Y, Qin L, Zhang P, Li K, Liang L, Sun J, Xu B, Dai Y, Li X, Zhang C, et al. Longitudinal COVID-19 profiling associates IL-1RA and IL-10 with disease severity and RANTES with mild disease. *JCI Insight*. 2020;5(13):e139834.
 71. Coutinho LL, Oliveira CN, Albuquerque PL, Mota SM, Meneses GC, Martins AM, Junior GB, Clementino MA, Gondim RN, Havt A, et al. Elevated IL-18 predicts poor prognosis in critically ill COVID-19 patients at a Brazilian hospital in 2020–21. *Future Microbiol*. 2022;17:1287–94.
 72. Nasser SMT, Rana AA, Doffinger R, Kafizas A, Khan TA, Nasser S. Elevated free interleukin-18 associated with severity and mortality in prospective cohort study of 206 hospitalised COVID-19 patients. *Intensive Care Med* Exp. 2023;11:9.
 73. Tjan LH, Furukawa K, Nagano T, Kiriu T, Nishimura M, Arii J, Hino Y, Iwata S, Nishimura Y, Mori Y. Early Differences in Cytokine Production by Severity of Coronavirus Disease 2019. *J Infect Dis*. 2021;223:1145–9.
 74. Liang S, Bao C, Yang Z, Liu S, Sun Y, Cao W, Wang T, Schwantes-An TH, Choy JS, Naidu S, et al. SARS-CoV-2 spike protein induces IL-18-mediated cardiopulmonary inflammation via reduced mitophagy. *Signal Transduct Target Ther*. 2023;8:108.
 75. Coperchini F, Chiovato L, Croce L, Magri F, Rotondi M. The cytokine storm in COVID-19: An overview of the involvement of the chemokine/chemokine-receptor system. *Cytokine Growth Factor Rev*. 2020;53:25–32.
 76. Hotchkiss RS, Monneret G, Payen D. Sepsis-induced immunosuppression: from cellular dysfunctions to immunotherapy. *Nat Rev Immunol*. 2013;13:862–74.
 77. Samson M, Nicolas B, Ciudad M, Greigert H, Guilhem A, Cladiere C, Straub C, Blot M, Piroth L, Rogier T, et al. T-cell immune response predicts the risk

- of critical SARS-Cov2 infection in hospitalized COVID-19 patients. *Eur J Intern Med.* 2022;102:104–9.
78. Pourgholaminejad A, Pahlavanneshan S, Basiri M. COVID-19 immunopathology with emphasis on Th17 response and cell-based immunomodulation therapy: Potential targets and challenges. *Scand J Immunol.* 2022;95: e13131.
 79. De Biasi S, Meschiari M, Gibellini L, Bellinazzi C, Borella R, Fidanza L, Gozzi L, Iannone A, Lo Tartaro D, Mattioli M, et al. Marked T cell activation, senescence, exhaustion and skewing towards TH17 in patients with COVID-19 pneumonia. *Nat Commun.* 2020;11:3434.
 80. Xu Z, Shi L, Wang Y, Zhang J, Huang L, Zhang C, Liu S, Zhao P, Liu H, Zhu L, et al. Pathological findings of COVID-19 associated with acute respiratory distress syndrome. *Lancet Respir Med.* 2020;8:420–2.
 81. Wu D, Yang XO. TH17 responses in cytokine storm of COVID-19: An emerging target of JAK2 inhibitor Fedratinib. *J Microbiol Immunol Infect.* 2020;53:368–70.
 82. Zhu D, Tian J, Wu X, Li M, Tang X, Rui K, Guo H, Ma J, Xu H, Wang S. G-MDSC-derived exosomes attenuate collagen-induced arthritis by impairing Th1 and Th17 cell responses. *Biochim Biophys Acta Mol Basis Dis.* 2019;1865: 165540.
 83. Honardoost MA, Naghavian R, Ahmadinejad F, Hosseini A, Ghaedi K. Integrative computational mRNA-miRNA interaction analyses of the autoimmune-deregulated miRNAs and well-known Th17 differentiation regulators: An attempt to discover new potential miRNAs involved in Th17 differentiation. *Gene.* 2015;572:153–62.
 84. Hou W, Kang HS, Kim BS. Th17 cells enhance viral persistence and inhibit T cell cytotoxicity in a model of chronic virus infection. *J Exp Med.* 2009;206:313–28.
 85. Lee J, Heo J, Kang H. miR-92b-3p-TSC1 axis is critical for mTOR signaling-mediated vascular smooth muscle cell proliferation induced by hypoxia. *Cell Death Differ.* 2019;26:1782–95.
 86. Bartel S, La Grutta S, Cilluffo G, Perconti G, Bongiovanni A, Giallongo A, Behrends J, Kruppa J, Hermann S, Chiang D, et al. Human airway epithelial extracellular vesicle miRNA signature is altered upon asthma development. *Allergy.* 2020;75:346–56.

Publisher's Note

Springer Nature remains neutral with regard to jurisdictional claims in published maps and institutional affiliations.